

RESEARCH ARTICLE

Novel Semisolid Design Based on Bismuth Oxide (Bi_2O_3) nanoparticles for radiation protection

Hamid Shirkhanloo¹; Mostafa Saffari²; Seyed Mohammad Amini³; Mehdi Rashidi^{4*}

¹Industry Health Research Institute (IPIHRI), Occupational and Environmental Health Research Center (OEHRC), PIHO, Tehran, Iran

²Department of Medical Nanotechnology, Islamic Azad University of pharmaceutical sciences (IAUPS), Tehran, Iran

³Radiation Biology Research Center, Iran University of Medical Sciences (IUMS), Tehran, Iran

⁴Department of Medical Nanotechnology, Islamic Azad University of pharmaceutical sciences (IAUPS), Tehran, Iran

ARTICLE INFO

Article History:

Received 29 October 2017

Accepted 07 December 2017

Published 28 December 2017

Keywords:

X-ray Protection

X-ray Absorbance

Semisolid

Bismuth Oxide Nanoparticles

Radiotherapy

Radiology

ABSTRACT

Objective(s): The dangerous effects of X-ray have been elucidated by scientific studies in occupational health hygiene. X-ray protective like an apron, thyroid shield and gloves have been made of lead (Pb) to protect against X-ray. However, such equipment makes a lot of safety and health problems such as toxicity, weight, inflexibility and troubles usage in a physician. To overcome such problems, X-ray absorbance's such as semi-solids have been developed. Here in, an investigation was carried out to see whether the mixture of semi-solid material containing bismuth oxide nanoparticles.

Methods: The mixture of semi-solid containing bismuth oxide nanoparticles was prepared based on the synthesis of bismuth oxide nanoparticles and formulation of semisolid. The bismuth oxide nanoparticles were prepared via synthesis method intermediating sorbitol with optimized conditions. In X-ray dosimeter test, the protective effect of bismuth oxide nanoparticles in semisolid was evaluated in comparison to lead adsorbents when all conditions were similar ($P < 0.05$).

Results: X-ray absorbance efficiency of bismuth nanoparticles dispersed in semisolids was more efficient than conventional lead absorbance. The percentage of X-ray absorption in the ointment of bismuth oxide nanoparticles is 56.79 while the absorption value in the 0.5-millimeter lead is between 40% and 42%.

Conclusions: The X-ray absorbent based on semi-solid containing bismuth oxide nanoparticles has many advantages in comparison to conventional lead absorbent such as; high surface area, low amount of sorbent, easy usage, high efficiency of X-ray absorbance, and lower toxic effect on the environment.

How to cite this article

Shirkhanloo H, Saffari M, Amini S M, Rashidi M, Novel Semisolid Design Based on Bismuth Oxide (Bi_2O_3) nanoparticles for radiation protection, *Nanomed Res J*, 2017; 2(4):230-238. DOI: 10.22034/nmrj.2017.04.004

INTRODUCTION

The amount of the risks from low doses of radiation is one of the central questions in radiological protection. It is particularly important when discussing the justification and optimization of diagnostic medical exposures. Medical application of X-rays can undoubtedly offer extensive benefits

in the healthcare of patients, but not without exposing them to harmful doses ranging from a few micro sieverts to a few tens of milli sievert [1]. Ionizing radiation was generated from the different source, the primary beam that only gets into the patient and indirectly via scattering radiation that exposed patients and medical staff. Also, there are a

* Corresponding Author Email: mehdi.rashidi1366@gmail.com

lot of natural X-rays in the environment that came from many different sources. The average radiation exposure to individuals is 6.2 micro sievert per year by natural background and medical imaging. High dose exposure of X-rays can cause adverse health effects, so, personal protective equipment such as lead aprons, thyroid shields, and lead glasses was used during X-ray fluoroscopy [2, 3]. Expanding the risk awareness of ionizing radiation exposure has led to several changes in practical protocols of medical X-ray Imaging. Lead with high density and high Z number is a good shield against gamma and X-ray radiation. Currently, lead aprons were used for patients and medical staff protection. However, usage of lead has some disadvantages due to heavyweight, lead aprons and many discomforts for medical staff [4] as well it is expensive and very toxic to the environment [5]. Therefore, production of environmentally friendly, non-toxic and lead-free radiation shields which provide less weight compared to conventional lead-based shields seem to be a difficult matter in radiation protection techniques [6].

The science and technology that imply the materials, structures, and engineering systems which is smaller than 100 nm in diameter are referred as nanotechnology. In these scales, materials represent unique properties that do not exist in bulk materials [7, 8]. Nanotechnology has been used for many diagnostic [9-11] and therapeutic in medical application [12, 13]. Many nanomaterials were introduced for radiation protection, regarding complex and efficient properties of nanoparticle with high Z values; they seem to be potent ingredients to diminish X-ray risks. Among different elemental combination, bismuth oxide has enough electromagnetic capacity in its electron levels to absorb and attenuate X-ray energy [14]. Zinc oxide and titanium oxide nanoparticles are widely used in medical and cosmeceutical application for UV ray protection in semisolid forms such as skin cream [15]. Bi₂S₃ nanoparticles have been introduced as an X-ray computed tomography imaging agent [16]. Bismuth also was used in polymer composite-based shielding materials and shown high capability in radiation shielding [14]. Here in we investigate design and development of semisolid material based on bismuth oxide nanoparticles (SSM-BONPs) with X-ray absorbance capability that could be useful

for X-ray protection skin cream. Experimental parameters affecting the X-ray absorbance such as temperature, size, thickness and semisolid dosage were studied and optimized.

MATERIALS AND METHODS

Materials

Bismuth nitrate (CAS N: 383074) and sorbitol (CAS N: 50-70-4) were purchased from Sigma Aldrich. A Pb (II) standard stock solution (1000 mg L⁻¹ in 1% nitric acid, 250 mL) was purchased from Fluka, Buchs, Switzerland. All other reagents were purchased from Merck (Darmstadt, Germany). All aqueous solutions were prepared with ultra-pure deionized water ($R \geq 18 \text{ M}\Omega \text{ cm}^{-1}$) from Milli-Q plus water purification system (Millipore, Bedford, MA, USA). Glassware's was washed with aqua regia and rinse out with deionized water.

Bismuth Oxide Nanoparticles Synthesis

Bismuth oxide nanoparticles were prepared by solid dispersion evaporation technique (SDAT) with sorbitol as carrier solutions. Briefly, 5 g of solid bismuth nitrate [Bi (NO₃).5H₂O] dissolve in a 0.92 ml sorbitol and 2 m DI water and stirred for 20 min at room temperature followed by sonication at 25 °C in an ultrasonic bath (40 kHz and 100 W). The mixture was diluted with 10 ml of distilled water and put on heater magnet stirrer plate for another 30 min. The pH of the sample solution was optimized up to 7, and no precipitation occurred during processes. The sample was dried in oven 90–110°C for 1h. Samples were placed in a furnace at 550–600°C. After 1-hour yellow sediment was formed [17-19]

Bismuth Oxide Semisolid preparation

150mg of hydroxypropyl methylcellulose (HPMC) (Merck Chemicals) was added to 1.5ml DI water in 80°C. The Same volume of 20°C water was injected into above solution which leads to homogenous gel. Under vigorous shaking 7gr of prepared Bi₂O₃ nanoparticles was completely dispersed into the gel. This semisolid contains 70% w/w Bi₂O₃ nanoparticles. With the same procedure, similar semisolids were prepared by glycerin (Merck chemicals), and eucerin (Merck chemicals) instead of HPMC. Another semisolid with bismuth nitrate instead of bismuth oxide nanoparticles were prepared as a control sample. Finally, the ceramic

powder was blended to make a semisolid texture qualitatively similar to semisolid which was used for radiation protection from human's hands [20-22].

Radiation protection measurements

An appropriate standard was used for assessing X-ray absorption by using environmental scintillation detector (ASP, E-600, RM-25, USA). In this standard, an X-ray tube and a detector were used which were 1000mm apart. X-ray absorbents samples were placed 500mm apart from the detector and the tube. In this method, X-ray absorbents with 0.5mm thickness were used. X-ray tube has opened a pore with a one-centimeter aperture which is created by two lead bricks and embedded in the front of the X-ray tube collimator. Probe detector is also placed inside a lead cylinder with a thickness of 2mm, and it is connected to a scintillation detector. All X-ray measurements were taken "with" and "without" the samples placed between the X-ray source and the detector based on Mallahi et al. study. Statistical significance of the data was analyzed by Single factorial analysis of variance (ANOVA) using Statistical Package for Social Sciences software version 10.0 (SPSS 10.0). The significance level was set at $p < 0.05$. The following formula was applied for X-ray attenuation measurements [14]:

$$\text{Attenuation(\%)} = \frac{\text{Electrometer reading without sample} - \text{Electrometer reading with}}{\text{Electrometer reading without sample}} \times 100$$

Apparatus and characterization methods

The morphology of the sorbent was examined using scanning electron microscopy (SEM, Phillips, PW3710) and transmission electron microscopy (TEM, CM30, Philips). X-ray diffraction (XRD) patterns for Bi_2O_3 nanoparticles and a mixture of Bi_2O_3 - semisolid were recorded by a GBC MMA diffractometer with beryllium-filtered Cu K α radiation (1.55Å) operating at 35.3kV and 30mA. The viscosity of Bi_2O_3 nanoparticles was measured with a viscometer (Brookfield, model: DV-III Ultra, SR: 0.01-250 RPM, USA). Viscosity appears in units of centipoise (cP) or milliPascal-seconds (mPas). The Geiger-Mueller (Anton Model 201 End Window GM Tube) detectors fulfill a wide variety of radiation measurement needs.

RESULTS AND DISCUSSION

Three Standards with different measurement geometries for radiation protection materials

has been introduced. Astm F2547-06 proposes a setup where the distance from the X-ray tube focal spot to the detector is 1000mm, with the radiation attenuation material positioned 500mm from the focal spot. This is referred to as "narrow beam geometry," and does not include the effects of secondary radiation from the attenuation material (scatter and fluorescence) in the measurement. This second element is significant when using Pb radiation protection garment [23]. The DIN 6857 standard proposes "inverse broad beam geometry," where the radiation attenuation material is mounted directly behind a 0.5mm thick Pb orifice and the detector is mounted directly behind this material. Measurements made in this geometry include scatter and fluorescence from the radiation attenuation material. After that, an absorbent of 0.5mm semisolid was used which we will refer to the geometry where the attenuating material is approximately half way between the X-ray focal spot and the detector as narrow beam geometry, and where the attenuation material is sandwiched between an orifice and the detector as "broad beam geometry [23].

Bismuth oxide nanoparticles characterizations

The results of synthesis of Bismuth oxide nanoparticles have been obtained in a series of scanning electron microscope (SEM) and transmission electron microscopy (TEM) micrographs. It was clarified that these particles are lower than 100 nanometers in size. The TEM micrographs have been demonstrated in fig. 1 (a, b). These micrographs characterize the size and spherical shape of the nanoparticles while SEM micrographs show the morphology. They can also be observed in fig. 2(a, b).

XRD pattern of synthesized bismuth oxide nanoparticles at 550-600°C was presented in fig 3, there is sharp peak located at $2\theta \approx 28^\circ$, as well two other intense lines at 33° and 46° . These lines reflect respectively to BiO, $\beta\text{-Bi}_2\text{O}_3$ modification, Bi_2O_3 , and Bi based on previous studies [24, 25].

Evaluation of X-ray intensity

The intensity of X-ray for dosimetric system scintillation probe for tube potentials 50–150 kV is presented in fig. 4. X-ray Intensity rate had been evaluated in three phases: In the first phase of the experiment, the intensity of the X-ray has

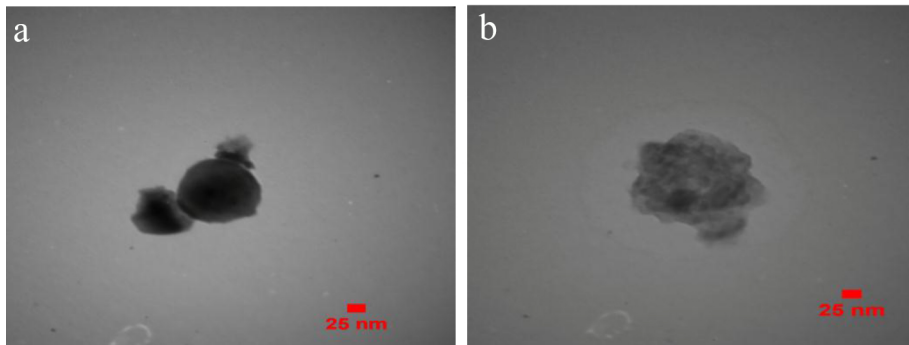


Fig. 1. a) TEM micrographs of the nanoparticles calcined at 550°C.
b) TEM micrographs of the nanoparticles calcined at 550 °C.

been examined using by ointment consists of bismuth oxides nanoparticles. In this experiment, the ointment is located 50 centimeters away from the tube center of X-ray, and 50 centimeters away from the detector [23]. Then, the amounts of X-ray to the ointment are demonstrated when entering, exiting and arriving at the detector, which has been taken the average after 7 repetitions. The second phase was conducted with X-ray radiation using no absorbent in order to understand the primary rate of radiation (Control group); so if we divide it by the intensity if X-ray absorbed by ointment of lead, the intensity rate of each can be gained. The third phase has been carried out using 0.5-millimeter lead as a standard comparison with the ointment. In this phase, the radiation with X-ray has also repeated 7

times, and the X-ray absorption was shown in fig 4. In all these phases of X-ray radiation, the intensity of radiation was measured on the scale of micro sievert per hour. The results showed that the powders of bismuth nanoparticles had better absorption than, bulk bismuth ointment and lead powder [26]. By dividing the average of ointment absorption by absorption without ointment, the passing percentage can be determined. This rate is equal to 56.79%, compared to 0.5-millimeter lead which has the absorption of 41.5%. Based on the findings, the percentage of X-ray absorption in the ointment of bismuth oxide nanoparticles is 56.79 while the absorption rate in the 0.5-millimeter lead is between 40% and 42%. In all the analysis, the same energy regarding kilovolt has been used.

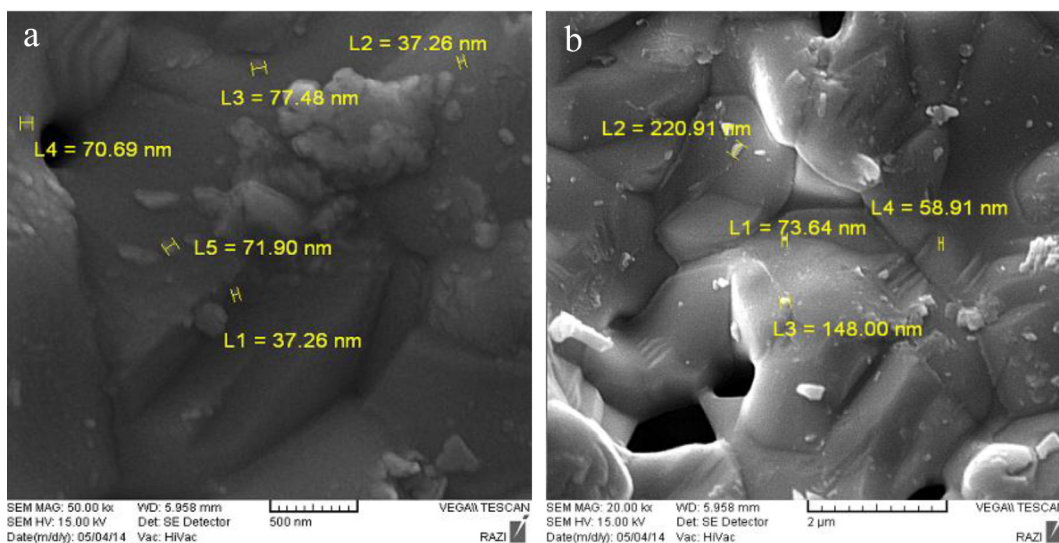


Fig. 2. a) SEM micrographs of Bi₂O₃ Nano powders are 37.26-77.48 nm in size at 550 °C.
b) SEM micrographs of Bi₂O₃ Nano powders are 58.91-220.91 nm in size at 550 °C.

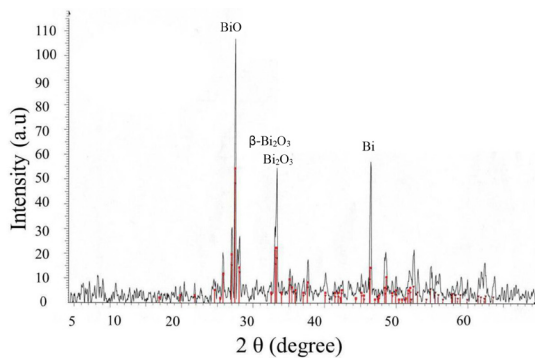


Fig. 3. Characterization of X-ray crystallography (XRD) of Bi_2O_3 powders calcined at 550-600°C

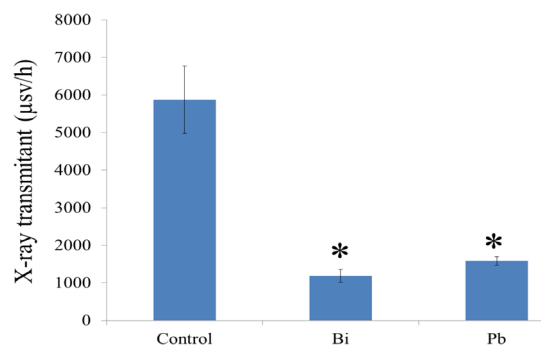


Fig. 4. The data are expressed as the mean \pm SD, n=3; *p<0.05

Semisolid viscosity test analysis

The viscosity of different formulation of prepared semisolids was investigated:

Formula 1: In formula 1 which is semi-solid containing HPMC with water, as shown in fig. 5 as the cutting speed increases, the viscosity of the sample decreases; this is the characteristic of semi-solid formulations with plastic-like features. Since there is HPMC in the formulation 1, as the cutting speed increases, polymer filaments are aligned with each other and the flow resistance decreases which is clear in the below figs. However, despite the high percentage of solid-phase of metal oxide in made semi-solid, the observed pseudo-plastic behavior will not be in full compliance with the relevant exponential curve and will show its individual behavior. As observed here, over the speed of 300 per second or 100rpm, the viscosity reaches a plateau that this point is probably the same time alignment of all the polymer filaments.

Formula 2: In formula 2 which containing organodimethicone and eucerin viscosity are high, almost in a basic phase and there is high resistance against the flow which is justifiable considering the high percentage of solid-phase of metal oxide in this formulation (fig. 6). After that, basic phase viscosity reaches its minimum and the stable amount which can be seen in stress curve against cutting speed. As indicated in the fig, the above curve fully follows the line and is compatible with high correlation (R approximately equal to 0.97). Semi-solid of sample 2 indicates 2162 stress and 10.7 viscosities, regarding the delayed first phase. According to what has been said, the behaviors of semi-solid 2 can be considered as plastic behavior. Based on the observations, the distributive of the above semi-

solid is evaluated as appropriate which is consistent with the data and interpretation of viscometer test. **Formula 3:** Formula 3 (fig. 7) which containing glycerin and cold-cream, the viscosity is high almost in a basic phase, and there is high resistance against the flow which is justifiable considering the high percentage of solid-phase of metal oxide in formulation 3.

After that basic phase, viscosity reaches its minimum and the stable amount which can be seen in stress curve against cutting speed. As indicated in the fig, the above curve completely follows the line and is compatible with high correlation. Semi-solid of sample 3 indicates 1.5 viscosities in the middle stages of the viscometer. According to what has been said, the behaviors of semi-solid 3 can be considered as plastic behavior. Although this behavior is not complete and even plastic behavior, and it was not completely homogeneous during the test. Based on the observations, the distributive of the above semi-solid is evaluated as rather appropriate which is consistent with the data and interpretation of viscometer test. Comparing to other semi-solid materials, an ointment made of eucerin does not form two-phase mode and it also has more stability and good shelf-life.

The designed X-ray absorbent can absorb X-ray in a great amount, however many absorbents have been made so far that can be compared to the designed absorbent. The designed X-ray absorbent is comprised of bismuth oxide nanoparticles and its advantage over its bigger-sized sample is that it has a high surface to volume ratio [27]. The results showed that in equal conditions, including an equal amount of lead, nano-lead or nano-lead sulfate has more beam attenuation power than normal

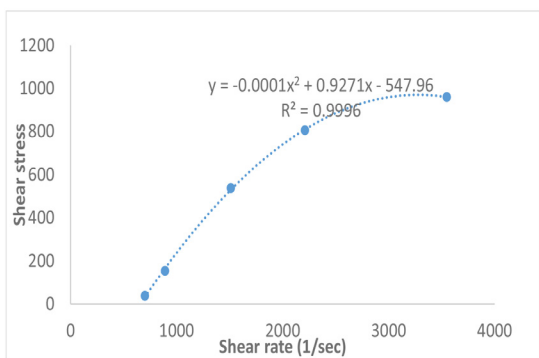


Fig. 5. profile viscosity of Sample F1: Semi-Solid Containing HPMC with Water (data are the average of 3 repetitions/replications).

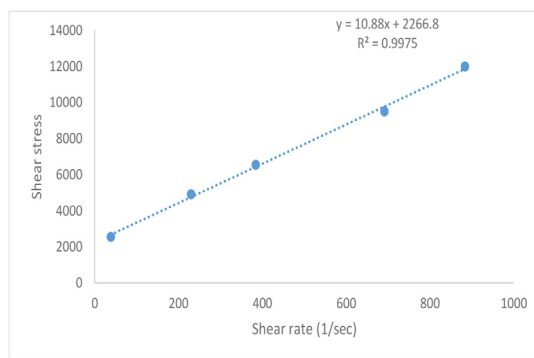


Fig. 6. Profile viscosity of sample F2: Containing organo-dimethicone and eucerin.

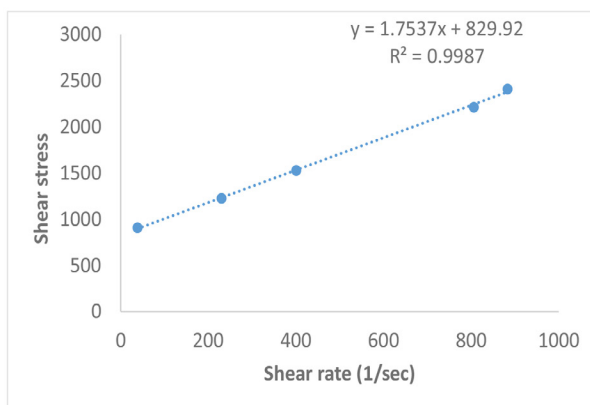


Fig. 7. Profile viscosity glycerol sample F3: Containing glycerin and cold-cream.

lead or lead sulfate in high energy. Comparing the designed X-ray absorbent semi-solid with X-ray absorbents like lead has indicated that bismuth with 0.5mm thickness can absorb 56.79% of X-ray, while lead absorbs 41.5%. Despite the fact that member's hand is completely insensitive to issues of X-ray protection and since this semi-solid could absorb 0.5mm ray, it shows that bismuth oxide nanoparticles could easily cover gonads because the maximum lead thickness for gonad protection is 0.5mm. Numerous studies have shown the X-ray attenuation increases with high atomic number elements.

Recently modern radiation protection gloves were developed for orthopedic surgeons, but lower the surgeon's tactile sensation and dexterity prevents its comprehensive use (ref glove). The novel radiation protective lotion that can be applied in a way like sun-block lotion could solve mentioned problems. Shah et al. developed a lotion that effectively

decreases radiation exposure up to 80% and does not affect tactile sensation and dexterity.[6] This lotion consists of an aqueous organic carrier and 75 weight % of bismuth oxide (Bi_2O_3) ceramic powder. The organic carrier comprises lubricants, humectants and surfactants such as glycerin, glycol sterate and polyethylene glycol sterate, and emulsifiers such as glycerol sterate. The ceramic powder was a mixture to lotion with a creamy texture qualitatively similar to hand lotions [6].

Our ointment consists of 70% weight of bismuth oxide nanoparticles and two other substances used as an additive ointment. So the proposed X-ray absorbent is contained bismuth oxide nanoparticles instead of bulk bismuth oxide and it provides a higher surface to volume ratio in comparison to X-ray absorbent ointment with bulk bismuth oxide. A protective glove made of natural rubber with shielding effect against X-ray composed of non-lead material was developed by Kamusella et al.

Gloves are flexible as result of elastic latex. The glove represents a lead equivalence value of 0.03-0.04mm Pb. Manufacturers declare that the attenuation of the primary radiation is 20%-25% at 80 kVp, as well as the scattered radiation of 52%-58% at 60 kVp and 42%-48% at 80 kVp in phantom. The shield gloves are slightly thicker and firmer in comparison to old sterile gloves [28]. In recent years, gloves have been made from bismuth which could absorb X-ray up to 55% in maximum 60 kVp, while the semi-solid absorbent could absorb X-ray to 56.79% with the difference that semi-solid is easily rubbed on hands and could be easily washed off, it also does not have sterling problems, but the gloves lower the skills of the surgeon and have sterling problems [29]. In another study by McCaffrey et al. conducted in 2006, there was a comparison between shields with and without lead [30]. This comparison which was made between different metals including cadmium, indium, tin, antimony, cesium, barium, cerium, gadolinium, tungsten, lead, and bismuth showed that metals with the high atomic number and low density create the best attenuation. Moreover, among seven compared shields, those containing tin and barium had low weight but appropriate attenuation (equal to 0.5mm lead) in 60-100 kVp [2]. The comparison of lead and tungsten shields indicated that those with pure tungsten in 100-120 kVp have better photon attenuation comparing to pure lead shields [26]. In another study conducted by Schlattl et al. in the same area compared lead aprons with aprons containing tin and aprons containing 80% tin and 20% bismuth. In their study, three categories of the beam with 75, 60, and 120 kVp were used. The comparison between the three covers showed that the cover containing tin had less attenuation than the other two types and the cover containing tin and bismuth slightly increases the surface dose [31]. The major difference between bismuth oxide nanoparticles and its bulk sample is that with a small amount of nanostructures there could be much absorption since surface to volume ratio increases and the amount of raw material is saved [26]. The sterile protective glove made of natural rubber has a shielding effect against diffuse X-ray radiation by the use of the non-lead material. Elastic latex keeps the glove flexible, The lead equivalence value of the glove is 0.03-0.04mm Pb. Under test situation of the manufacturer, the attenuation of the primary radiation of 20%-25%

at 80kVp, as well as the scattered radiation of 52%-58% at 60kVp and 42%-48% at 80kVp is shown for the Phantom. Compared to conventional sterile gloves, the protective gloves are slightly thicker and firmer. After the intervention, an idea of the examiner was requested for calculation of the sense of touch. This was actually to show whether there was an important limit with the protective glove in relation to the beat of the inguinal artery and the handling of the materials [28]. There is another type of double-layer gloves containing X-ray absorbents material, these gloves are heavier than other gloves and could not solve the problem of their heaviness and inflexibility and still have a sterling problem [29]. But the advantage of semi-solid over gloves and similar cases is that they are single-use gloves and are easily washed off hands. Based on the studies mentioned above and the safety data sheet, bismuth oxide nanoparticles could be easily used, although more investigation is recommended. In 2013, researchers made an X-ray absorbent color from non-lead materials which could absorb rays up to 80% and was made of trioxide tungsten, since it has high density; it can absorb X-ray better and works better than lead [32]. But still extracting and providing tungsten is not economical compared to lead. There have been some studies on the biocompatibility of bismuth which showed that it does not create environmental problems due to its low toxicity and is not accumulated in the body, while lead is harmful to environment and human health [2]. For instance, fuel consumption causes lead release through car exhaust and easily enters the digestive and respiratory system and infect the body and are highly carcinogenic. The same problem is also true about experimental tools which distribute lead particles that enter the human body and develop fatal cancers.

CONCLUSIONS

Lead with a high atomic number is easily used in all X-ray protective devices, thyroid shields and so on. In the present study, bismuth nano-oxide was used as an X-ray absorbent. This absorbent had many advantages like high absorption level, less consumption, and less cost, and therefore is a good substitute for lead. Nano bismuth makes less harm to human health and is better than lead in terms of safety and toxicity. The ointment produced which consists of bismuth oxide nanoparticles can be

easily applied in healthcare centers like operation rooms and minimizes the risk of X-ray. Finally, it was shown that novel semisolid made of Bi_2O_3 has the potential to effectively attenuate X-rays (primary and phantom-scattered) generated during imaging in the operating room rather than lead so that it can be considered as a protective material during these procedures.

CONFLICTS OF INTEREST

The authors declare that they have no conflict of interest.

REFERENCES

1. Wall B, Kendall G, Edwards A, Bouffler S, Muirhead C, Meara J. What are the risks from medical X-rays and other low dose radiation? *The British Journal of Radiology*, 2006;79 (940):285-294.
2. Aghamiri M, Mortazavi S, Tayebi M, Mosleh-Shirazi M, Baharvand H, Tavakkoli-Golpayegani A, Zeinali-Rafsanjani B. A novel design for production of efficient flexible lead-free shields against X-ray photons in diagnostic energy range. *Journal of Biomedical Physics and Engineering*, 2011;1 (1 Dec).
3. Abdollahi H, Shiri I, Atashzar M, Sarebani M, Moloudi K, Samadian H. Radiation protection and secondary cancer prevention using biological radioprotectors in radiotherapy. *International Journal of Cancer Therapy and Oncology*, 2015;3 (3).
4. Fontainha CC, Baptista N, Annibal T, Faria LO. Radiation shielding with Bi_2O_3 and ZrO_2 : Y composites: preparation and characterization.
5. Hulbert SM, Carlson KA. Is lead dust within nuclear medicine departments a hazard to pediatric patients? *Journal of nuclear medicine technology*, 2009;37 (3):170-172.
6. Shaw S, Chen K, Mejia A. Radiation protection to surgeons' hands with a novel radiation attenuating lotion. *AAOS Annual Meeting: Scientific SE39*; 2012.
7. Amini SM, Gilaki M, Karchani M. Safety of nanotechnology in food industries. *Electronic physician*, 2014;6 (4):962.
8. Samadian H, Mobasheri H, Hasanpour S, Majid RF. Needleless Electrospinning System, an Efficient Platform to Fabricate Carbon Nanofibers. *Journal of Nano Research*. Vol 50: Trans Tech Publ; 2017:78-89.
9. Fatemi F, Amini SM, Kharrazi S, Rasaei MJ, Mazlomi MA, Asadi-Ghalehni M, Rajabibazl M, Sadroddiny E. Construction of genetically engineered M13K07 helper phage for simultaneous phage display of gold binding peptide 1 and nuclear matrix protein 22 ScFv antibody. *Colloids and Surfaces B: Biointerfaces*, 2017;159 (Supplement C):770-780.
10. Emami T, Madani R, Golchinfar F, Shoushtary A, Amini SM. Comparison of Gold Nanoparticle Conjugated Secondary Antibody with Non-Gold Secondary Antibody in an ELISA Kit Model. *Monoclonal antibodies in immunodiagnosis and immunotherapy*, 2015;34 (5):366-370.
11. Samadian H, Mobasheri H, Hasanpour S, Faridi Majidi R. Electrospinning of polyacrylonitrile nanofibers and simulation of electric field via finite element method. *Nanomedicine Research Journal*, 2017;2 (2):87-92.
12. Amini SM, Kharrazi S, Jaafari MR. Radio frequency hyperthermia of cancerous cells with gold nanoclusters: an in vitro investigation. *Gold Bulletin*, 2017;50 (1):43-50.
13. Amini SM, Kharrazi S, Hadizadeh M, Fateh M, Saber R. Effect of gold nanoparticles on photodynamic efficiency of 5-aminolevulinic acid photosensitizer in epidermal carcinoma cell line: an in vitro study. *IET Nanobiotechnology*
14. Nambiar S, Osei EK, Yeow JT. Polymer nanocomposite-based shielding against diagnostic X-rays. *Journal of Applied Polymer Science*, 2013;127 (6):4939-4946.
15. Smijs TG, Pavel S. Titanium dioxide and zinc oxide nanoparticles in sunscreens: focus on their safety and effectiveness. *Nanotechnology, science and applications*, 2011;4:95.
16. Rabin O, Perez JM, Grimm J, Wojtkiewicz G, Weissleder R. An X-ray computed tomography imaging agent based on long-circulating bismuth sulphide nanoparticles. *Nature materials*, 2006;5 (2):118.
17. Jha R, Pasricha R, Ravi V. Synthesis of bismuth oxide nanoparticles using bismuth nitrate and urea. *Ceramics international*, 2005;31 (3):495-497.
18. Anilkumar M, Pasricha R, Ravi V. Synthesis of bismuth oxide nanoparticles by citrate gel method. *Ceramics international*, 2005;31 (6):889-891.
19. Patil M, Deshpande V, Dhage S, Ravi V. Synthesis of bismuth oxide nanoparticles at 100 C. *Materials letters*, 2005;59 (19):2523-2525.
20. Premjeet S, Ajay B, Sunil K, Bhawana K, Sahil K, Divashish R, Sudeep B. Additives in topical dosage forms. *International Journal of Pharmaceutical, Chemical, and Biological Sciences*, 2012;2:78-96.
21. Visscher M, Davis J, Wickett R. Effect of topical treatments on irritant hand dermatitis in health care workers. *American journal of infection control*, 2009;37 (10):842. e841-842. e811.
22. Lu P-J, Huang S-C, Chen Y-P, Chiueh L-C, Shih DY-C. Analysis of titanium dioxide and zinc oxide nanoparticles in cosmetics. *Journal of food and drug analysis*, 2015;23 (3):587-594.
23. McCaffrey J, Tessier F, Shen H. Radiation shielding materials and radiation scatter effects for interventional radiology (IR)

- physicians. *Medical physics*, 2012;39 (7):4537-4546.
24. Leontie L, Caraman M, Alexe M, Harnagea C. Structural and optical characteristics of bismuth oxide thin films. *Surface Science*, 2002;507-510 (Supplement C):480-485.
25. Mädler L, Pratsinis SE. Bismuth Oxide Nanoparticles by Flame Spray Pyrolysis. *Journal of the American Ceramic Society*, 2002;85 (7):1713-1718.
26. Azman NN, Siddiqui S, Hart R, Low I-M. Effect of particle size, filler loadings and x-ray tube voltage on the transmitted x-ray transmission in tungsten oxide—epoxy composites. *Applied Radiation and Isotopes*, 2013;71 (1):62-67.
27. Botelho M, Künzel R, Okuno E, Levenhagen RS, Basegio T, Bergmann CP. X-ray transmission through nanostructured and microstructured CuO materials. *Applied Radiation and Isotopes*, 2011;69 (2):527-530.
28. Kamusella P, Scheer F, Lüdtke CW, Wiggermann P, Wissgott C, Andresen R. Interventional Angiography: Radiation Protection for the Examiner by using Lead-free Gloves. *Journal of clinical and diagnostic research: JCDR*, 2017;11 (7):TC26.
29. Shah S, Chen K, Mejia A. Radiation protection to surgeons' hands with a novel radiation attenuating lotion. *AAOS Annual Meeting: Scientific SE39*; 2012.
30. McCaffrey J, Shen H, Downton B, Mainegra-Hing E. Radiation attenuation by lead and nonlead materials used in radiation shielding garments. *Medical physics*, 2007;34 (2):530-537.
31. Schlattl H, Zankl M, Eder H, Hoeschen C. Shielding properties of lead-free protective clothing and their impact on radiation doses. *Medical physics*, 2007;34 (11):4270-4280.
32. Movahedi MM, Abdi A, Mehdizadeh A, Dehghan N, Heidari E, Masumi Y, Abbaszadeh M. Novel paint design based on nanopowder to protection against X and gamma rays. *Indian journal of nuclear medicine: IJNM: the official journal of the Society of Nuclear Medicine, India*, 2014;29 (1):18.